Asian Journal of Chemistry; Vol. 26, No. 18 (2014), 5991-5994

ASIAN JOURNAL OF CHEMISTRY

http://dx.doi.org/10.14233/ajchem.2014.16406

Some Novel Phases in Binary System of $PbO-Sb_2O_3$

H. GÜZIN ASLAN

Erciyes University Faculty of Arts, Department of Chemistry, 38039 Melikgazi, Kayseri, Turkey

Corresponding author: Fax: +90 352 4374933; Tel: +90 352 4374901-33167; E-mail: guzina@erciyes.edu.tr

Received: 21 September 2013; *Accepted*: 4 April 2014; *Published online*: 1 September 2014; AJC-15838

In this study, we have investigated the $PbO-Sb_2O_3$ binary system. PbO and Sb_2O_3 are reacted using different stoichiometric ratios at 650 °C in an air using a gold and a platinum reaction vessel by heating for 24 h. $PbSb_2O_6$, $Pb_9Sb_8O_{21}$, $Pb_4Sb_2O_8$, $Pb_9Sb_8O_{17}$, $Pb_6Sb_2O_{11}$, $Pb_5Sb_2O_9$, $Pb_7Sb_2O_{11}$, $Pb_8Sb_2O_{12}$, $Pb_9Sb_2O_{13}$, phases are synthesized and these phases 0.5, 0.692, 0.8, 0.818, 0.857, 0.87, 0.875, 0.88, 0.9 mole fractions, respectively. Reaction products are characterized by the X-ray powder diffraction and by DTA/TG analysis methods.

Keywords: Antimony trioxide, Lead oxide.

INTRODUCTION

The mechanochemical ceramic method of preparing oxide powders involves mechanical process. In this method of approach, yields powders are suitable for particle size below 100 nm. However, even single phase powders of mixed oxides remain chemically inhomogeneous after mechanical processing (≤ 10 min). The crystalline compound differs in composition from the starting mixture and amorphous component. Although these difficulties, solid electrolytes are important components of solid state electrochemical devices, which are becoming increasingly important for use in energy conversion, chemical processing sensing and combustion control. Hence, many researchers have investigated the solid state reactions in the binary system of antimony and lead sesquioxides. Some stoichiometric compounds such as $PbSb_2O_6$[1-6], Sb_2O_4[2], $Pb_2Sb_2O_{11}$[3], PbO[7], $Pb_{(3+x)}Sb_2O_8$[6-8], $Pb_3Sb_2O_{8.47}$[8], $PbO{\cdot}Sb_2O_6$[9], $Pb_2Sb_2O_7$[9], $3PbO{\cdot}Sb_2O_3$[9], $Pb_4Sb_2O_9$[9] are being known to occur. However, information about the $PbO-Sb_2O_3$ system in the presence of air, which is an important constituent of the complete ternary system, is extremely limited and contradictory.

For this reason, we are prepared 55 different mixtures. $PbO-Sb_2O_3$ are reacted different stoichiometric ratios at 650 °C in air using gold and platinum vessel. These substances are characterized with XRD and DTA/TG methods.

EXPERIMENTAL

The powder samples in this study are prepared by mixing PbO (99.99 %) and Sb_2O_3 (99.99 %) Merck without further purification. The solid mixture that contained a different amount of PbO doping (χ: $n_{PbO}/n_{PbO} + nSb_2O_3$) are prepared. Mixing and homogenation are performed in an agate morter. These oxide mixtures are calcified in a furnace in platinum crucibles in air at 650-1000 °C for 24 h. After the heat treatment procedure, fine powder samples are slowly cooled in the furnace by switching it off (uncontrolled). The colour of the compounds is observed to change from light yellow to dark yellow.

Powder diffraction data of the samples are determined using a XRD analyses with Bruker AXS D8 advanced diffractometer and a Bragg-Brentano geometry with graphite monochromator. CuKα radiation operated at 40 kV and 40 mA. The divergence and receiving slits of 1 and 0.1 mm, respectively are located on the diffractometer. Diffraction patterns are scanned by steps 0,002° (2θ) over the angle range of 10-90 (2θ). Diffracted beams are counted with a NaI (Tl) scintillation detector and the obtained XRD data are compared with the reference data. Thermal measurements are taken using a simultaneous DTA/TG system (Schimadzu DT-40 type). The specimens, usually 7 mg in mass, are heated at a rate of 10 °C min^{-1} from room temperature to 1000 °C. Measurement is taken in dynamic air atmosphere using a platinum sample holder and an αAl_2O_3 inert reference substance.

RESULTS AND DISCUSSION

Several nonstoichiometric antimony oxides such as Sb_2O_3, Sb_2O_4 and Sb_2O_5 have been widely used in various industries[10,11]. Sb_2O_3 typically has two polymorphs, cubic polymorph (senarmontite, stable phase) and orthorhombic polymorph (valentinite, metastable phase) and the orthorhombic polymorph

can be transformed into the cubic one at 490-530 °C[12]. Senarmontite has long been used as an additive to enhance the flame retardancy of polymer resins, whereas valentinite has not due to its undesirable oxidization when exposed to air or sunlight[13]. Senarmontite is shown to act as a catalyst in combination with vanadium for the selective oxidation of *o*-xylene[14]. Valentinite decomposes giving endothermic peak about 1120 °C with a slight loss weight. In this investigation, all the diffraction peaks are indexed in orthorhombic crystal system and unit cell parameters are calculated as (a) 5.440, (b) 4.802. and (c) 11.760 Å. Valentinite (Sb_2O_3) is a major component of the Sb_2O_3-B_2O_3 binary glasses possessing nonlinear optical properties[15]. The orthorhombic α and monoclinic β forms are the two polymorps of Sb_2O_4. The orthorhombic Sb_2O_4 with unit cell dimensions of (a) 546, (b) 482 and (c) 1182 pm can be formed by the oxidation reaction of cubic Sb_2O_3 at 600 °C for 24 h[16,17]. The PbO compound has an orthorhombic crystal symmetry with (a) 549, (b) 589.2, (c) 475.2 pm. The orthorhombic phase of PbO is stable above 500 °C, the red form (litharge tetragonal) is stable below 500 °C.

PbO compound has a orthorombic crystal symmetry with (a) 5.4903, (b) 5.8920, (c) 4.7520. The orthorombic phase of PbO is stable above 500 °C. The red form (litharge tetragonal) is stable below 500 °C.

Obtained phases are indexed and calculated. Their unit cell parameters and some physical parameters are shown the PbO-Sb_2O_3 system in Table-1.

TABLE-1
OBSERVED PHASES IN THE SYSTEM OF (PbO-Sb_2O_3)

Comp.	Crystal system	Unit parameters (pm)
$PbSb_2O_6$	Hexagonal	(a) 531 (b) 538
$Pb_9Sb_8O_{21}$	Orthorhombic	(a) 1392 (b) 1295 (c) 1001
$Pb_4Sb_2O_8$	Monoclinic	(a) 1358.9 (b) 1223.5 (c) 928.3 β: 9826.5
$Pb_9Sb_8O_{17}$	Monoclinic	(a) 1361.9 (b) 1221.6 (c) 929.2 β: 9845.2
$Pb_6Sb_2O_{10}$	Monoclinic	(a) 1364.2 (b) 1225.6 (c) 934.7 β: 9831.3
$Pb_5Sb_2O_9$	Monoclinic	(a) 1365.9 (b) 1225.6 (c) 940.1 β: 9843.9
$Pb_7Sb_2O_{11}$	Monoclinic	(a) 1365.0 (b) 1222.6 (c) 936.8 β: 9831.1
$Pb_8Sb_2O_{12}$	Monoclinic	(a) 1363.4 (b) 1223.1 (c) 934.5 β: 9825.8
$Pb_9Sb_2O_{13}$	Monoclinic	(a) 13.654 (b) 12.234 (c) 9.379 β: 9831.5

$0.1 \leq \chi \leq 0.5$ region: In the two-phase region, the powder patterns of the samples are indexed in two crystal systems that are orthorhombic and hexagonal. The Sb_2O_4 phase is orthorhombic and $PbSb_2O_6$ (0.5 mole fraction) is hexagonal with (a) 531 and (b) 538 pm. Twenty six mixtures are studied in this area $PbSb_2O_6$ X-ray diagram is shown in Fig. 1. The $PbSb_2O_6$ + Sb_2O_4 heterogenous mixture's X-ray diagram is shown in Fig. 2 (some diffraction lines which belong to Sb_2O_4 are assigned with (+) symbols in the powder patterns). These results also shown in Fig. 10.

According to the $PbSb_2O_6$ DTA/TG diagram in Fig. 3, the endotherm at 300 °C, accompanied by a weight loss of 3 % is due to water removal. After removal of water, the net weight loss at 684.72 °C is 2 % in second step with one endothermic peak, which corresponds to reduction of the $Pb_2Sb_2O_6$ phase;

$$Pb_2Sb_2O_6 \rightarrow Pb_2Sb_2O_5 + ½O_2$$

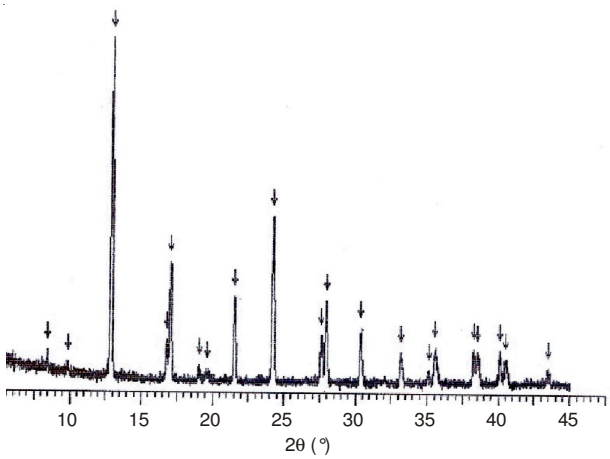

Fig. 1. XRD patterns of $PbSb_2O_6$ after heating 650 °C

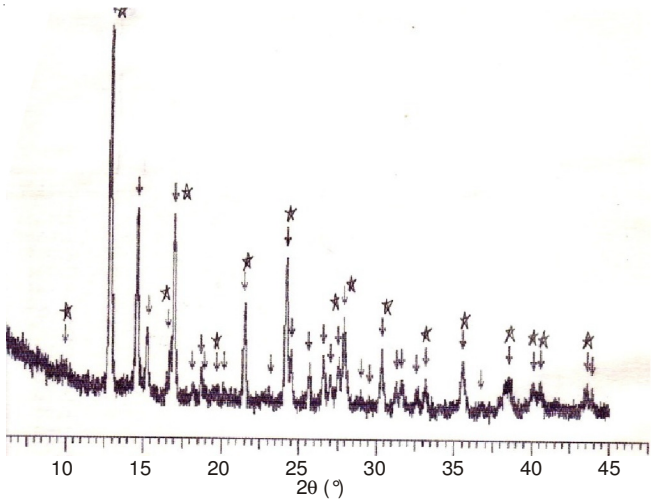

Fig. 2. XRD patterns of Sb_2O_4 + $PbSb_2O_6$ heterogene mixture after heating 650 °C (Sb_2O_4 peaks marked*)

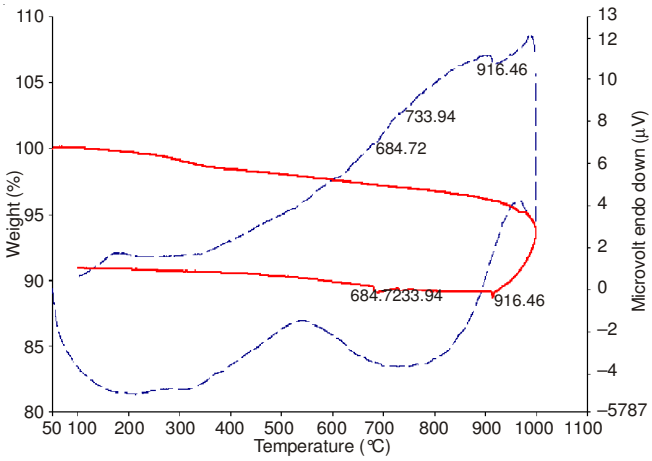

Fig. 3. Measured DTA/TG diagrams of $PbSb_2O_6$

The weight loss by 916.46 °C is 5 % in third step with one endothermic peak, which corresponds to the reduction of the $Pb_2Sb_2O_5$ phase;

$$Pb_2Sb_2O_5 \rightarrow Pb_2Sb_2O_4 + ½\ O_2$$

0.5-0.8 mol fraction: This area included that $PbSb_2O_6$ + $Pb_9Sb_8O_{21}$ heterogenous mixture. $Pb_9Sb_8O_{21}$ (0.691 mole fraction) is orthorhombic with (a) 1392, (b) 1295, (c) 1001

pm and X-ray diagram shown in Fig. 4. Thermal behaviour of this area is almost same. All compounds in this area is thermally stable. These compounds hasn't got any endothermic or exothermic peaks and any weight loss. As a sample of this area DTA/TG diagram ($Pb_9Sb_8O_{21}$) is shown in Fig. 5. As a sample of the $PbSb_2O_6$ + $Pb_9Sb_8O_{21}$ heterogenous mixture is located in Fig. 6 (some diffraction lines which belong to $PbSb_2O_6$ are assigned with (+) symbols in the powder patterns). Twenty mixture are studied in this area. These results also given in Fig. 10.

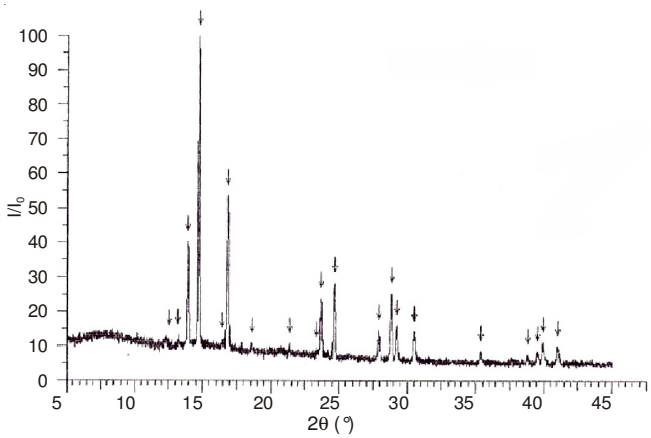

Fig. 4. XRD patterns of $Pb_9Sb_8O_{21}$ after heating at 650 °C

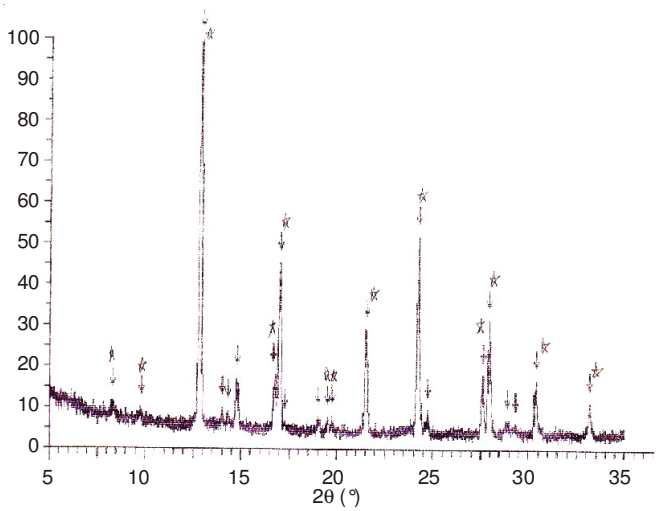

Fig. 5. XRD patterns of $Pb_9Sb_8O_{21}$ + $PbSb_2O_6$ heterogene mixture after heating at 650 °C ($PbSb_2O_6$ peaks marked*)

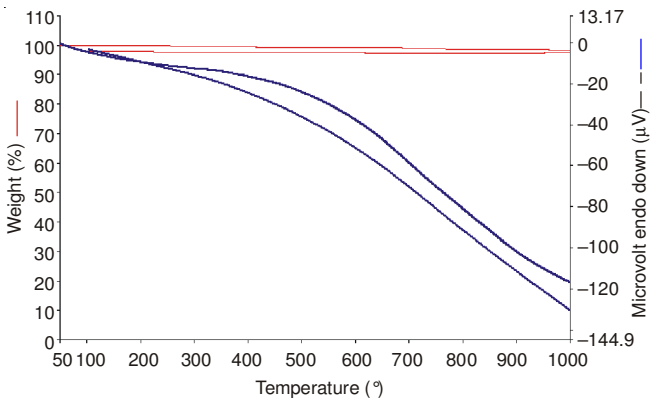

Fig. 6. Measured DTA/TG diagrams of $Pb_9Sb_8O_{21}$

0.8-0.9 Mole fraction: The 0.8-0.9 mole fraction is included solid solution area. As a sample of this area the $Pb_6Sb_2O_{11}$ (0.857 mole fraction) compound is monoclinic with (a) 13.589, (b) 12.256, (c) 9.347 β: 98.313 and the X-ray diffraction pattern is shown in Fig. 7. Seven mixtures are studied in this area and all phases were indexed with the same lattice constants. These results are located in graphical abstract. Dependence of the lattice constans of solid solutions area with the mol ratio is predicted in Fig. 8.

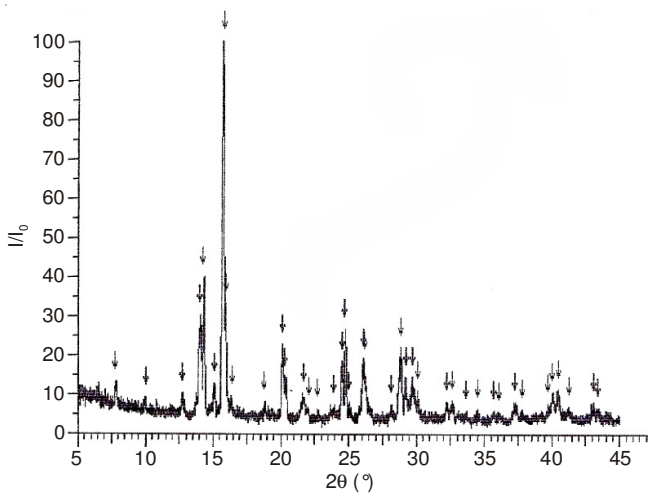

Fig. 7. XRD patterns of $Pb_6Sb_2O_{11}$ after heating at 650 °C

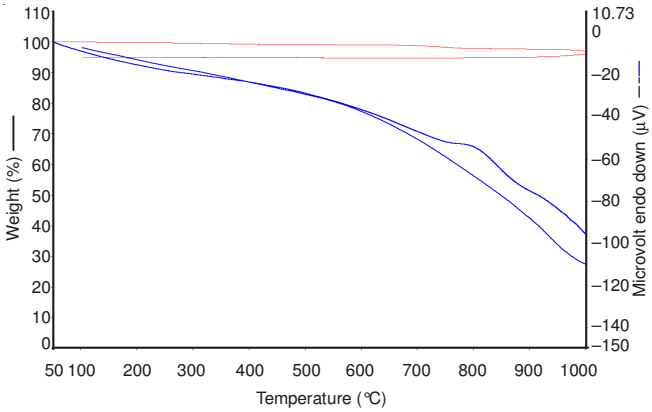

Fig. 8. Measured DTA/TG diagrams of $Pb_6Sb_2O_{11}$

TG/DTA analysis for this area is recorded in nitrogen atmosphere from 25 to 1025 °C. Thermal behavior of this area is almost same. All compounds in this area is thermally stable. These compounds hasn't got any endothermic or exothermic peaks and any weight loss. As a sample of this area DTA/TG diagram($Pb_6Sb_2O_{11}$) is shown in Fig. 9. Seven mixtures are studied in this area (Fig. 10).

Conclusion

In conclusion, new phases in PbO-Sb_2O_3 mixtured synthesized. All new phases were characterized by X-ray powder diffraction and DTA/TG methods. Between 0.1-0.9 mole fraction was detected three region. These region were 0.1-0.5, 0.5-0.8 and 0.8- 0.9, respectively. In 0.1- 0.5 region, the powder patterns of the samples were indexed in two crystal systems that were orthorhombic (Sb_2O_4) and hexagonal

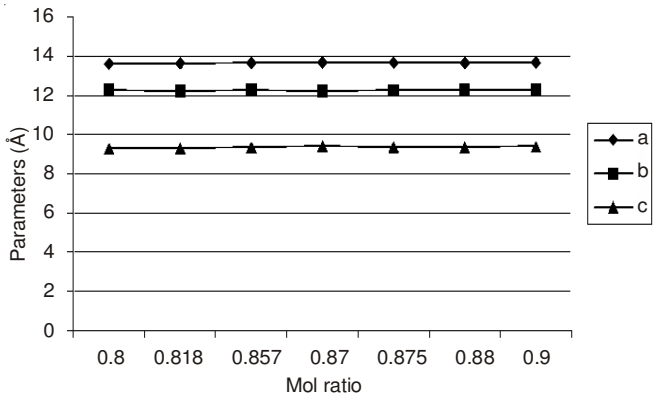

Fig. 9. Dependence of the lattice constans of solid solutions area with the mol ratio

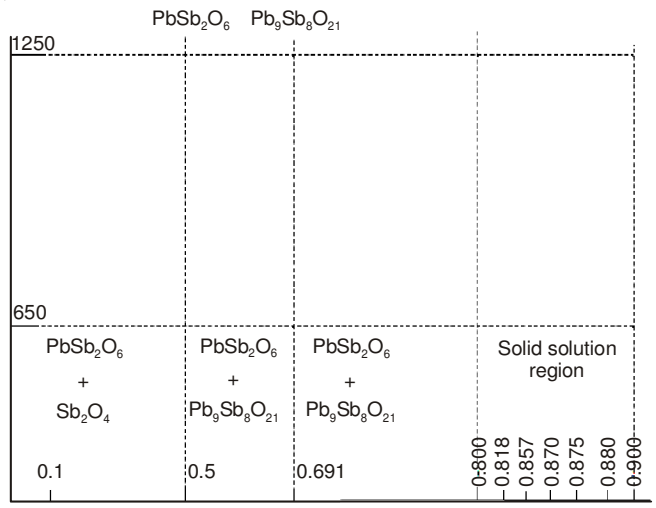

Fig. 10. Phase diagram of PbO-Sb_2O_3 binary system

($PbSb_2O_6$). In 0.5- 0.8 mole region, $PbSb_2O_6$ + $Pb_9Sb_8O_{21}$ heterogenous mixture was detected. $PbSb_2O_6$ (0.5 mole fraction) was hexagonal and $Pb_9Sb_8O_{21}$ was orthorhombic. The 0.8-0.9 mole fraction was included solid solution area. As a sample of this area the $Pb_6Sb_2O_{11}$ (0.857 mole fraction) compound was monoclinic with (a) 13.589, (b) 12.256, (c) 9.347 β: 98.313. Further research in this area is in progress in our laboratory.

ACKNOWLEDGEMENTS

The authors are grateful to Erciyes University's Research Foundation for financial support.

REFERENCES

1. R.J. Hill, *J. Solid State Chem.*, **71**, 12 (1987).
2. S.S. Lopatin, E.S. Medvedev and I.P. Raevskii, *Russ. J. Inorg. Chem.*, **30**, 867 (1985).
3. A.A. Bush and Y.N. Venetsev, *Russ. J. Inorg. Chem.*, **31**, 769 (1986).
4. F. Raymande, Spectroscopie Moleculaire, (Acad. Sci. Press, Paris) p. 274 (1972).
5. A. Magneli, *Arkiu för Khimii*, *Minerolojioch Geoloji Band*, 15B No:3.
6. A.V. Astafev, A.N. Bush, S.Y. Stefanovich and Y.N. Venetsev, *Neorgan. Meter. Izv. Akad. Nauk SSSR [Khim]*, 645 (1984).
7. G. Burchard and W Z. Rudorrf, *Z. Anorgan. Allgem. Chem.*, **447**, 149 (1978).
8. V.G. Kuznetsov and R.A. Koz'min, *Zh. Neorg. Khim*, **10**, 2361 (1958).
9. D.C. Gelach, R.W. Hennig and D.A. Pawlek, *Metallography*, 2215 (1968).
10. J. Hu, T.W. Odom and C.M. Lieber, *Acc. Chem. Res.*, **32**, 435 (1999).
11. Y.N. Xia, P.D. Yang, Y.G. Sun, Y.Y. Wu, B. Mayers, B. Gates, Y.D. Yin, F. Kim and H.Q. Yan, *Adv. Mater.*, **15**, 353 (2003).
12. A.E. Whitten, B. Dittrich, M.A. Spackman, P. Turner and T.C. Brown, *Dalton Trans.*, 23 (2004).
13. R.D. Bernett, A. Mitchell and T.C. Brown, *J. Mater. Sci.*, **39**, 1075 (2004).
14. J. Spengler, F. Anderle, E. Bosch, R.K. Grasselli, B. Pillep, P. Behrens, O.B. Lapina, A.A. Shubin, H.-J. Eberle and H. Knözinger, *J. Phys. Chem. B*, **105**, 10772 (2001).
15. K. Terashima, T. Hashimoto, T. Uchino, S.-H. Kim and T. Yoko, *Ceram. Soc. Japan*, **104**, 1008 (1996).
16. S.A. Nedil'ko and A.M. Sych, *Neorgan. Mater.*, **12**, 2014 (1976).
17. A. Tairi, J.C. Champarnaud-Mesjard, D. Mercurio and B. Frit, *Rev. Chim. Miner.*, **22**, 699 (1985).